Int. J. of Thermal & Environmental Engineering
Volume 20, No. 1 (2023) 29-33

Thermal Catalysis Effects of $Ca(NO_3)_2$, $Mg(NO_3)_2$, KNO_3, and $Fe(NO_3)_3$ on Olive Mill Solid Waste

Islam Alkahder and Reyad A. Shawabkeh*

Chemical Engineering Department, University of Jordan, Amman, Jordan

Abstract

Thermogravimetric Analysis - Differential Scanning Calorimetry (TGA-DSC) was employed in this study to investigate the thermal characteristics of olive mill solid waste (OMSW) both alone and in conjunction with six different compositions of $Ca(NO_3)_2$, $Mg(NO_3)_2$, KNO_3, and $Fe(NO_3)_3$. Emphasis was placed on assessing the impact of these compositions on the thermal behavior and heat flow. The analyses of TGA–DSC for the seven samples, conducted at a 10 K/min heating rate, revealed that the thermal decomposition of the OMSW occurred in three stages corresponding to the removal of water, devolatilization, and the formation of bio-char. Particularly noteworthy was the observation of complete combustion events between approximately 155°C and 240°C for four samples with distinct compositions during TGA testing. These findings underscore the significant influence of nitrate salt compositions on the thermal behavior of OMSW. The insights derived from this study contribute to the optimization of waste-to-energy processes and the refinement of thermal treatment protocols for sustainable OMSW management.

Keywords: *Thermogravimetric Analysis; Differential Scanning Calorimetry; Olive mill solid waste; Thermal behavior*

1. Introduction

The global olive industry generates significant amounts of olive mill solid waste (OMSW) annually, posing both environmental challenges and untapped resource potential. The escalating production of biomass waste, including agricultural residues like OMSW, emphasizes the need for careful disposal methods to prevent environmental contamination and associated health risks [1]. With over 800 million olive trees worldwide, primarily in Mediterranean countries like Spain and Greece, Jordan's 25 million olive trees contribute to an annual production of 220,000 tons of olives, 35,000 tons of olive oil, 60,000 tons of olive pomace, and an estimated 200,000 cubic meters of OMSW [2]. This surplus not only presents waste management challenges, but also offers a unique opportunity for sustainable energy exploration and waste-to-product conversion. Nitrate salts [3, 4], along with sulfate [4, 5], chloride [6, 7] and carbonate [7] salts, play a crucial role as a source of oxide catalysts in thermal treatment processes, notably in pyrolysis and gasification [8].

In the realm of thermochemical processes, this study expands its focus to unravel the catalytic dynamics inherent in metal nitrate salts during the Thermogravimetric Analysis Differential scanning calorimetry (TGA-DSC) of impregnated OMSW. Alkaline earth metal, including calcium, and magnesium in addition to potassium and iron are systematically explored for their catalytic prowess. The deliberate selection of nitrate salts is underpinned by their dual advantage—preventing catalyst poisoning and facilitating removal at lower temperatures during the pyrolysis process [8]. The catalytic strategy involving metal salt impregnation in OMSW emerges as a key area of investigation. This research intricately compares the TGA-DSC curves originating from diverse compositions of metal nitrate salt impregnations. The overarching goal is to contribute nuanced insights into how metal nitrate salts intricately shape the primary degradation mechanisms within impregnated OMSW, thereby bring more insight and comprehension of catalytic processes in the thermochemical conversion landscape.

2. Materials and Methods

The OMSW sample, obtained as dried blocks from a local mill in Jordan, underwent manual crushing. Subsequently, the crushed OMSW underwent a four-hour de-moisturization process in an oven set at 105ºC. Following this, the refined

* Corresponding author. Tel.: +962-6-5355000
E-mail: rshawabk@ju.edu.jo

DOI: 10.5383/ijtee.20.01.005

OMSW was further processed through a Jaw Crusher, and the resulting material was sieved to separate particles based on specific screen sizes of 0.35 mm. Six solutions with distinct compositions of calcium nitrate ($Ca(NO_3)_2 \cdot 4H_2O$), magnesium nitrate ($Mg(NO_3)_2 \cdot 6H_2O$), potassium nitrate (KNO_3), and iron nitrate ($Fe(NO_3)_3 \cdot 9H_2O$) were also prepared, each following the specific compositions detailed in Table 1. The wet impregnation method [9] was employed to introduce solutions of nitrate salts into the OMSW.

Table 1: Compositions and Mass Ratios of Nitrate Solutions for OMSW Impregnation

	$Ca(NO_3)_2 \cdot 4H_2O$	$Mg(NO_3)_2 \cdot 6H_2O$	KNO_3	$Fe(NO_3)_3 \cdot 9H_2O$	OMSW
1-OMSW	17.1	8.6	2.9	2.7	100
2-OMSW	147.5	22.4	7.5	35.4	100
3-OMSW	31.6	64.0	5.4	25.3	100
4-OMSW	31.6	16.0	21.5	25.3	100
5-OMSW	162.3	24.6	33.1	7.8	100
6-OMSW	36.0	73.0	24.5	5.8	100

2.1. Ultimate Analysis:

The elemental composition of the feedstock sample, encompassing carbon (C), nitrogen (N), hydrogen (H), sulfur (S), and oxygen (O), is revealed through the ultimate analysis. Additionally, the determination of ash or mineral matters (MM) content is deemed integral to proximate analysis. The CHNSO analysis was performed using the FLASH Organic Elemental Analyzer (model number 2000, USA) during the experimental procedure and following those reported in the work of Raza et al. [10] and Mazzoni et al. [11].

2.2. Proximate Analysis:

The Simultaneous TGA-DSC analysis, employed for various purposes in the study, including the investigation of the effect of nitrate salts on OMSW, and also utilized for the proximate analysis [12] of the raw OMSW. This analytical approach provides insights into the mass fractions of moisture, volatile matter, fixed carbon, and ash within the sample. The analysis is carried out using the STA TA instrument (model number Q600, USA) with a controlled heating rate of 10 K/min and following those reported by Raza et al. [10] and Janajreh et al. [13].

2.3. Calorific Analysis:

Calorific analysis plays a crucial role in establishing the energy balance of the feedstock. This procedure involves the use of the Parr compensated jacket calorimeter (model number 6100, USA). It includes placing the solid sample within an oxygen bomb, sealing it, and introducing oxygen. The sealed bomb is immersed in a continuously stirred purified water bath, with meticulous temperature monitoring to account for potential heat loss. Ignition of the sample in the presence of oxygen results in the generation and release of heat, a parameter meticulously recorded by the calorimeter. The precise determination of the heating value is achieved by integrating this recorded signal over time and considering the known mass of the feedstock.

2.4. TGA-DSC analysis:

OMSW characterization involved the use of a STA TA instrument (model number Q600, USA) with a controlled heating rate of 10 K/min. TGA was employed to profile thermal decomposition and determine moisture content, while DSC provided insights into associated heat changes during decomposition and combustion processes. These analyses, conducted with the specified instrument, contributed to a comprehensive understanding of the OMSW's thermal behavior for various applications.

3. Results and Discussion

3.1. Proximate, Ultimate, and Calorific Analysis:

The proximate analysis outcomes, outlined in Table 2, demonstrate that the results obtained for OMSW are consistent with the standard ranges for comparable waste materials within the olive industry [14-18]. These results imply that the substantial volatile matter content indicates a notable production of gaseous pyrolysis products [19]. Conversely, the heightened levels of fixed carbon and ash suggest that this portion is apt to produce solid char [19, 20].

The proximate analysis of OMSW provides valuable insights into its applicability for various purposes, especially in the realm of energy recovery. The recorded average moisture content of 6.45% signifies the material's relative dryness, rendering it suitable for solid fuel applications. A lower moisture content holds the potential to reduce tar density, optimize gasification efficiency, and increase energy content [20]. The substantial average volatile matter content, measured at 68.48%, emphasizes the presence of organic, combustible components, making OMSW well-suited for energy recovery processes like combustion or gasification, as higher volatile matter enhances flammability [21]. With an average fixed carbon content of 19.34%, OMSW contains a significant amount of stable carbonaceous material, offering potential value for energy generation.

Nevertheless, the observed ash content, averaging 5.72% and forming at around 500°C, presents challenges by potentially inducing slag formation within the furnace. This occurrence could hinder the efficiency of biomass gasification reactions, resulting in a decrease in syngas yield and negatively affecting syngas quality [22]. In summary, the results of the proximate analysis suggest that OMSW possesses promising attributes for energy recovery applications, particularly due to its low moisture content, high volatile matter, and substantial fixed carbon content. These combined characteristics position OMSW as a viable candidate for thermal conversion processes.

Table 2: Proximate analysis, ultimate analysis, and calorific value for OMSW.

Proximate analysis	Run 1	Run 2	Run 3	Mean
Moisture (Wt%)	6.12±0.01	6.28±0.01	6.96±0.01	6.45±0.01
Volatile (Wt%)	66.89±0.01	70.96±0.01	67.60±0.01	68.48±0.01
Fixed Carbon (Wt%)	20.14±0.01	18.15±0.01	19.74±0.01	19.34±0.01
Ash (Wt%)	6.85±0.05	4.61±0.05	5.70±0.05	5.72±0.01
Ultimate analysis	Run 1	Run 2	Run 3	Mean
C (Wt%)	49.59±0.01	50.18±0.01	49.5±0.01	49.76±0.01
O (Wt%)	43.71±0.01	43.06±0.01	43.94±0.01	43.57±0.01
H (Wt%)	6.58±0.01	6.66±0.01	6.46±0.01	6.57±0.01
N (Wt%)	0.02±0.01	0	0	0.01±0.01
S (Wt%)	0	0	0	0
HHV (MJ/kg)	23.48±0.1	23.3±0.1	24.47±0.1	23.75±0.2

*HHV: higher heating value

3.2. TGA-DSC Analysis:

The TGA-DSC curves for the seven samples are presented in Figs. 1 though 7, revealing distinct trends upon initial inspection of the TGA curves. Figs. 1 to 3 share a common pattern of at least three events, while Figs. 4 to 7 show only two events. Focusing on the results, the analysis begins with the raw OMSW depicted in Fig. 1. The TGA curve indicates four events: the first concludes around 180ºC, associated with demoisturization; the second concludes at approximately 330ºC, encompassing most of the devolatilization and pyrolysis reactions; and the third involves the decomposition of most of the fixed carbon, concluding at around 500ºC.

Examining the DSC curve Fig. 1, it reveals that the decomposition of OMSW is generally exothermic, characterized by two major exothermal peaks. The highest heat flow is observed at 14.44 W/g, occurring at 311ºC. These findings provide a comprehensive understanding of the thermal behavior of the raw OMSW, shedding light on the specific temperature ranges and corresponding events during the TGA-DSC analysis.

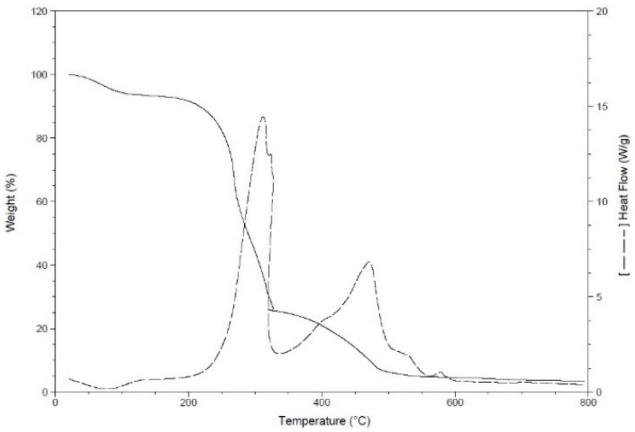

Fig. 1. TGA-DSC for OMSW

The addition of nitrate salts induces a significant alteration in thermal behavior. Through the TGA-DSC analysis of sample 1-OMSW, which is consists of a ratio of 17.1 $Ca(NO_3)_2{\cdot}4H_2O$: 8.6 $Mg(NO_3)_2{\cdot}6H_2O$: 2.9 KNO_3: 2.7$Fe(NO_3)_3{\cdot}9H_2O$: 100 OMSW, as depicted in Fig. 2, it becomes evident that the TGA events have undergone changes, resulting in the occurrence of two devolatilization events that extend to approximately 450ºC. This alteration plays a crucial role in the breakdown of organic compounds, subsequently leading to a heightened release of volatile gases [23]. Additionally, there is a modification in the heat flow, attributed to the effect of nitrate composition. The major peak of heat flow occurs around 450 ºC, extending the residence time of OMSW in the low-temperature range and enhancing volatile release. This observed phenomenon is closely associated with the extent of devolatilization observed in the TGA analysis [24].

As illustrated in Fig. 3, sample 2-OMSW exhibits a similar trend to 1-OMSW, with notable distinctions. The primary differences include a reduction in the maximum heat flow from approximately 15 W/g to 9 W/g. This decline is associated with the high mass ratio of nitrate salts, leading to a decrease in both the Higher Heating Value (HHV) and Lower Heating Value (LHV). Another significant contrast lies in the conclusion of the devolatilization event around 500ºC, indicating a more pronounced impact of the composition compared to 1-OMSW.

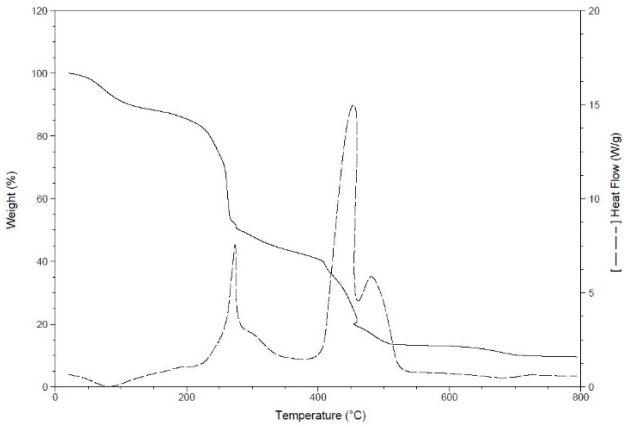

Fig. 2. TGA-DSC of 1-OMSW (17.1 [$Ca(NO_3)_2{\cdot}4H_2O$] : 8.6 [$Mg(NO_3)_2{\cdot}6H_2O$] : 2.9 [KNO_3] : 2.7 [$Fe(NO_3)_3{\cdot}9H_2O$] : 100 OMSW)

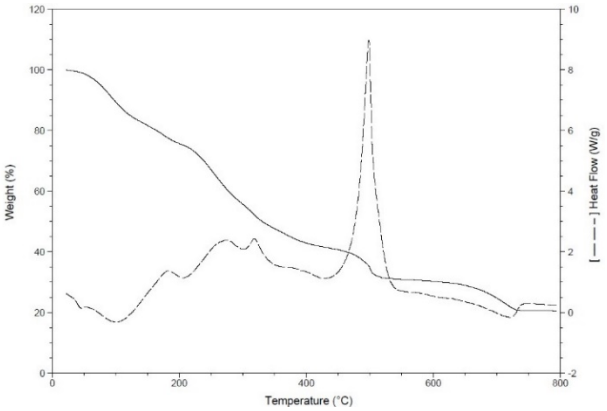

Fig. 3. TGA-DSC of 2-OMSW (147.5 [$Ca(NO_3)_2{\cdot}4H_2O$] : 22.4 [$Mg(NO_3)_2{\cdot}6H_2O$] : 7.5 [KNO_3] : 35.4 [$Fe(NO_3)_3{\cdot}9H_2O$] : 100 OMSW)

In the analysis of samples 3-OMSW, 4-OMSW, 5-OMSW, and 6-OMSW, the TGA-DSC curves, as shown in Figs. 4 to 7, sequentially, reveal a thorough combustion process occurring at relatively low temperatures. This phenomenon may be due to the catalytic influence, markedly lowering the ignition temperature. Additionally, the presence of oxygen from nitrate salts further contributes to this observed combustion at lower temperature.

One of the key factors contributing to this significant change in the trend is the increase in the magnesium nitrate or potassium nitrate ratio. The elevation in the calcium nitrate and iron nitrate to a very high ratio, as observed in sample 2-OMSW, does not have the same effect. Upon close examination of Figs. 4 to 7, differences in combustion temperatures are evident. Sample 6-OMSW exhibits combustion at the lowest temperature (155°C), followed by 4-OMSW at 160°C, 3-OMSW at 165°C, and 5-OMSW at approximately 235°C. These variations can be attributed to differences in the compositions of the nitrate salts.

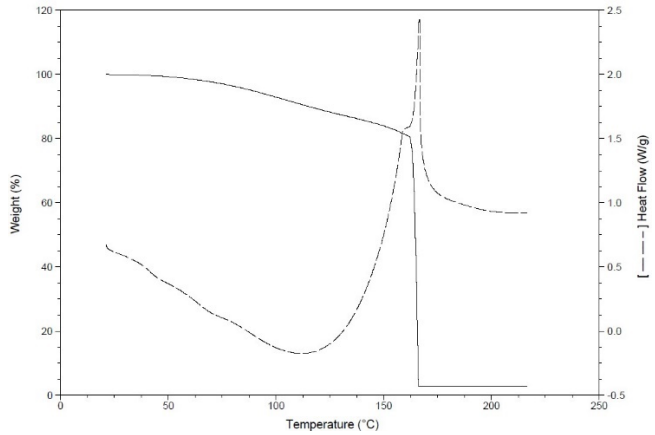

Fig. 4. TGA-DSC of 3-OMSW (31.6 [$Ca(NO_3)_2 \cdot 4H_2O$] : 64.0 [$Mg(NO_3)_2 \cdot 6H_2O$] : 5.4 [KNO_3] : 25.3 [$Fe(NO_3)_3 \cdot 9H_2O$] : 100 OMSW)

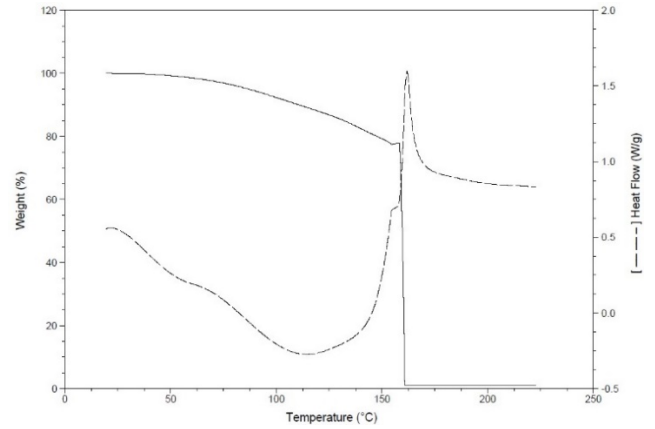

Fig. 5. TGA-DSC of 4-OMSW (31.6 [$Ca(NO_3)_2 \cdot 4H_2O$] : 16.0 [$Mg(NO_3)_2 \cdot 6H_2O$] : 21.5 [KNO_3] : 25.3 [$Fe(NO_3)_3 \cdot 9H_2O$] : 100 OMSW)

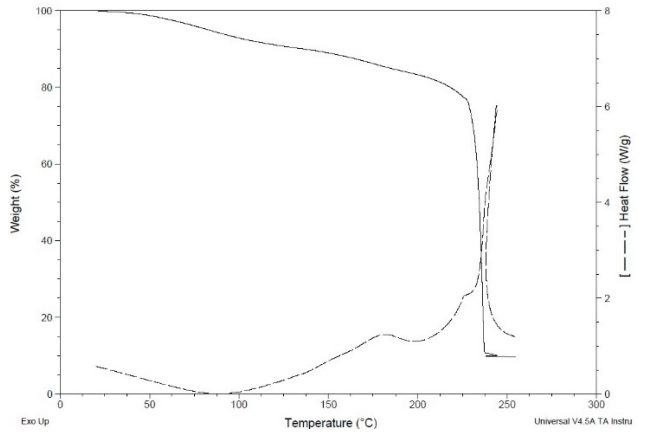

Fig. 6. TGA-DSC of 5-OMSW (162.3 [$Ca(NO_3)_2 \cdot 4H_2O$] : 24.6 [$Mg(NO_3)_2 \cdot 6H_2O$] : 33.1 [KNO_3] : 7.8 [$Fe(NO_3)_3 \cdot 9H_2O$] : 100 OMSW)

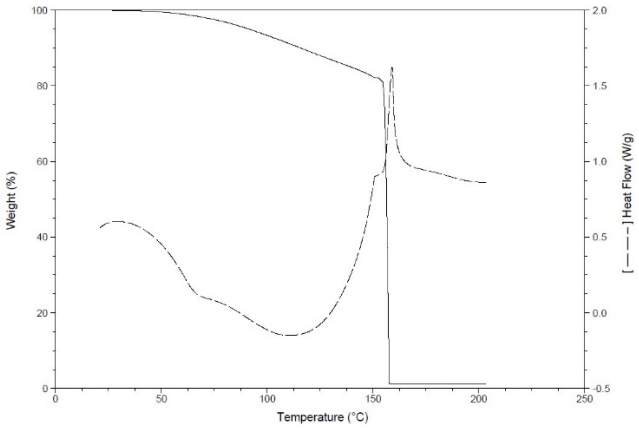

Fig. 7. TGA-DSC of 6-OMSW (36.0 [$Ca(NO_3)_2 \cdot 4H_2O$] : 73.0 [$Mg(NO_3)_2 \cdot 6H_2O$] : 24.5 [KNO_3] : 5.8 [$Fe(NO_3)_3 \cdot 9H_2O$] : 100 OMSW)

4. Conclusion

Summarizing, this study employed TGA-DSC to explore the thermal characteristics of OMSW and its interactions with various six different compositions of $Ca(NO_3)_2$, $Mg(NO_3)_2$, KNO_3, and $Fe(NO_3)_3$. The investigation, conducted at a 10 K/min heating rate, revealed a three-stage thermal decomposition of OMSW, involving water removal, devolatilization, and bio-char formation. Four samples exhibited clear combustion events between 155°C and 240°C, indicating a noteworthy impact of nitrate salt compositions on OMSW's thermal behavior. In addition, for the other two samples observable changes in TGA events, extended devolatilization, and shifts in heat flow underscored the breakdown of organic compounds and increased volatile gas release. Proximate, ultimate, and calorific analyses highlighted OMSW's potential for energy recovery, emphasizing its low moisture content, high volatile matter, and substantial fixed carbon. Challenges, such as ash content affecting biomass gasification reactions, were identified. In impregnated OMSW, varying nitrate salt compositions influenced combustion at lower temperatures, particularly due to magnesium and potassium nitrate ratios. This comprehensive investigation enhances our understanding of the complex interactions between OMSW and metal nitrate salts. It paved the way for informed decision-making in waste management and energy recovery strategies.

Acknowledgments

We acknowledge the collaboration received from Prof. Janajreh's group at Khalifa University, Abu Dhabi, UAE.

References

[1] Qureshi, T., Shoaib, H. M., Ali, U., Siddiqi, M. H., Hussain, M. A., and Lateef, H. U., Comparison of physio-chemical characteristics of different compost samples. International Journal of Thermal and Environmental Engineering, 2021. 18(1), 09–17.

[2] Khdair, A.I., G. Abu-Rumman, and S.I. Khdair, Pollution estimation from olive mills wastewater in Jordan. Heliyon, 2019. 5(8): p. e02386.

[3] Bru, K., et al., Pyrolysis of metal impregnated biomass: An innovative catalytic way to produce gas fuel. Journal of Analytical and Applied Pyrolysis, 2007. 78(2): p. 291-300.

[4] Terakado, O., A. Amano, and M. Hirasawa, Explosive degradation of woody biomass under the presence of metal nitrates. Journal of Analytical and Applied Pyrolysis, 2009. 85(1): p. 231-236.

[5] Dobele, G., et al., Application of catalysts for obtaining 1,6-anhydrosaccharides from cellulose and wood by fast pyrolysis. Journal of Analytical and Applied Pyrolysis, 2005. 74(1): p. 401-405.

[6] Branca, C., C. Di Blasi, and A. Galgano, Pyrolysis of Corncobs Catalyzed by Zinc Chloride for Furfural Production. Industrial & Engineering Chemistry Research, 2010. 49(20): p. 9743-9752.

[7] Di Blasi, C., A. Galgano, and C. Branca, Influences of the Chemical State of Alkaline Compounds and the Nature of Alkali Metal on Wood Pyrolysis. Industrial & Engineering Chemistry Research, 2009. 48(7): p. 3359-3369.

[8] Eibner, S., et al., Catalytic effect of metal nitrate salts during pyrolysis of impregnated biomass. Journal of analytical and applied pyrolysis, 2015. 113: p. 143-152.

[9] Saxena, R., et al., Nano-enhanced PCMs for low-temperature thermal energy storage systems and passive conditioning applications. Clean Technologies and Environmental Policy, 2021. 23.

[10] Raza, S.S., Elagroudy, S., Janajreh, I., Gasification of municipal solid waste: Thermodynamic equilibrium analysis using gibbs energy minimization method and CFD simulation of a downdraft gasifier, J. of Solid Waste Technology and Management, Vol.46.2, 2020.

[11] Mazzoni, L.,Janajreh, Elagroudy, Sherien I., Ghenai, C., Modeling of plasma and entrained flow co-gasification of MSW and petroleum sludge, Energy, Vol. 196, 2020.

[12] Adeyemi, I., et al., Gasification behavior of coal and woody biomass: Validation and parametrical study. Applied Energy, 2017. 185: p. 1007-1018.

[13] Janajreh, I., Adeyemi, I., Elagroudy, S., Gasification feasibility of polyethylene, polypropylene, polystyrene waste and their mixture: Experimental studies and modeling, Sustainable Energy Technologies and Assessments, Vol. 39, 2020.

[14] Volpe, M., et al., One stage olive mill waste streams valorisation via hydrothermal carbonisation. Waste Management, 2018. 80: p. 224-234.

[15] Dorado, F., et al., Fast pyrolysis as an alternative to the valorization of olive mill wastes. Journal of the Science of Food and Agriculture, 2021. 101(7): p. 2650-2658.

[16] Uzun, B.B., A.E. Pütün, and E. Pütün, Composition of products obtained via fast pyrolysis of olive-oil residue: effect of pyrolysis temperature. Journal of Analytical and Applied Pyrolysis, 2007. 79(1-2): p. 147-153.

[17] Zabaniotou, A., et al., Boosting circular economy and closing the loop in agriculture: Case study of a small-scale pyrolysis–biochar based system integrated in an olive farm in symbiosis with an olive mill. Environmental Development, 2015. 14: p. 22-36.

[18] Ouazzane, H., et al., Olive mill solid waste characterization and recycling opportunities: A review. J. Mater. Environ. Sci, 2017. 8(8): p. 2632-2650.

[19] García, G.B., et al., Characterization and modeling of pyrolysis of the two-phase olive mill solid waste. Fuel processing technology, 2014. 126: p. 104-111.

[20] Naryanto, R.F., et al., The effect of moisture content on the tar characteristic of wood pellet feedstock in a downdraft gasifier. Applied Sciences, 2020. 10(8): p. 2760.

[21] Sha, D., et al., Influence of Volatile Content on the Explosion Characteristics of Coal Dust. ACS Omega, 2021. 6(41): p. 27150-27157.

[22] Gao, Y., et al., Syngas Production from Biomass Gasification: Influences of Feedstock Properties, Reactor Type, and Reaction Parameters. ACS Omega, 2023. 8(35): p. 31620-31631.

[23] Mueangta, S., P. Kuchonthara, and S. Krerkkaiwan, Catalytic Steam Reforming of Biomass-Derived Tar over the Coal/Biomass Blended Char: Effect of Devolatilization Temperature and Biomass Type. Energy & Fuels, 2019. 33(4): p. 3290-3298.

[24] Chen, H., N.a. Liu, and W. Fan, Two-step Consecutive Reaction Model of Biomass Thermal Decomposition by DSC. Acta Physico-Chimica Sinica, 2006. 22(7): p. 786-790.